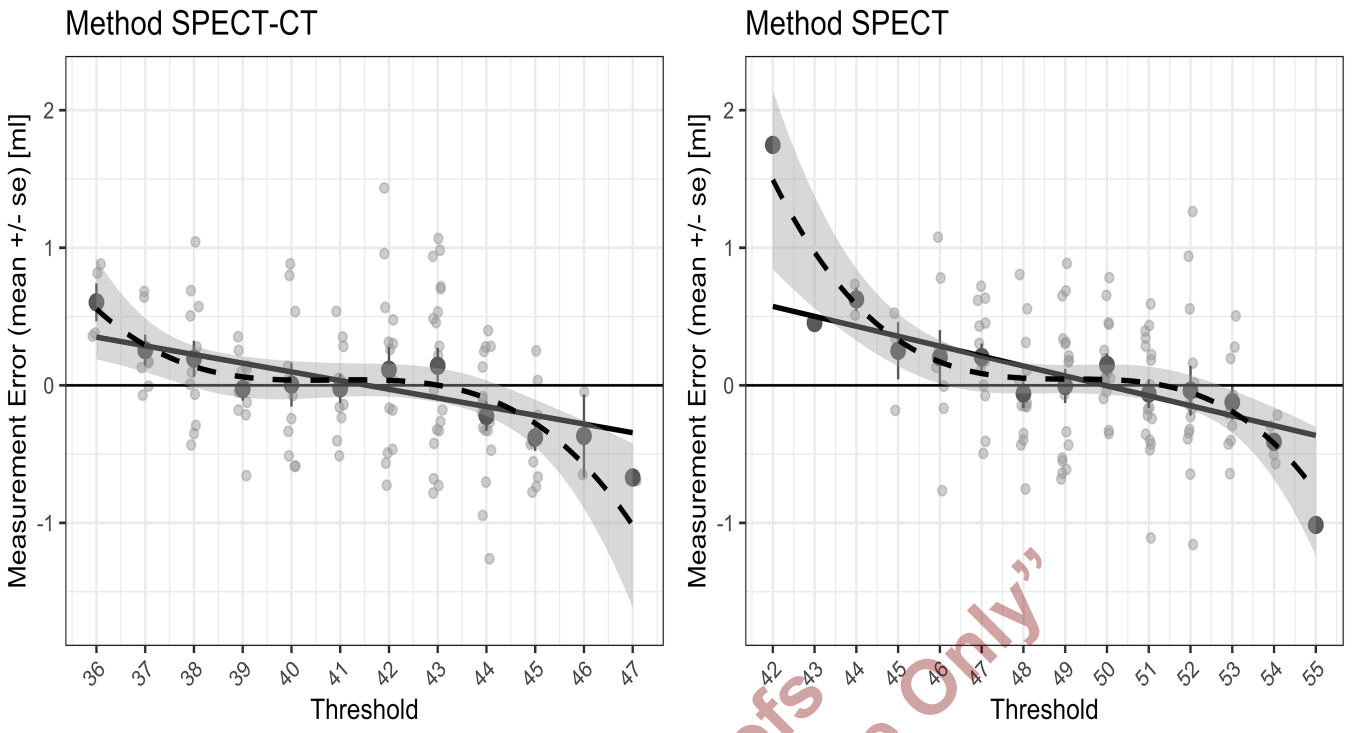

Fig. (4). Linear and spline regression models for the volume estimation error as a function of the threshold values. Single measurement errors (shaded dots), error mean and standard deviations (gray bold dots with bars), linear model (continuous black line) and spline model (dashed black line) with prediction interval (shaded area) are plotted. Do notice x-scales are different in the two panels.

2.4. Statistical analysis

Statistical analysis was performed using R software version 4.0.3. The Mean, Median, Standard Deviation (SD), Standard Error (SE), the Mean Absolute Percentage Error (MAPE) and the Root Mean-Square Error (RMSE) were computed for each method. Any difference in volume calculation from phantom studies between planar method, SPECT and SPECT-CT and the effective volume was evaluated by means of ANOVA and posthoc tests, and p-values are reported; where feasible, confidence intervals for measurement error were also computed.

2.5. Patient studies

From July 2019 to February 2021, a SPECT-CT protocol was performed in a total of 14 patients affected by hyperthyroidism. The hybrid image study was considered a useful tool for a better definition of the relationships with the adjacent anatomical structures, in addition to thyroid planar scintigraphy. Each patient received a fixed dose of 148 MBq of 99mTc-pertechnetate ($^{99m}TcO_4^-$). After 15 minutes, a thyroid image (zoom factor of 2), a mediastinal image and a SPECT-CT with the same acquisition parameters as the phantom studies mentioned above were acquired, respectively. Four patients were excluded from the study because the target volume was not optimally delineable in CT images (2 patients) or SPECT and SPECT-CT reconstructions (2 patients). Two patients were excluded due to the greater activity of the salivary glands compared to the thyroid tissue, not allowing the correct use of iso-contouring ROIs. Therefore only 8 patients (average age 59 years, age range 29-78 years, 5 male and 3 female) were considered eligible for the study. Four patients had solitary hot nodules and 4 Graves' Disease. One of the latter also had ectopic tissue developing caudally from the hyoid region and separated from the thyroid lobes. Each potential target volume was estimated using the planar, SPECT and SPECT-CT method, with CT as the reference. Only one expert clinician for each procedure, planar (L. C.), SPECT (E. C.), SPECT-CT (M. P.) and CT (P. B.) respectively, performed all the elaborations. In the patient with Basedow ectopic tissue, the calculation was performed on coronal slices to avoid that the iso-contouring ROIs included hyperfunctioning thyroid tissue. In all other cases, the ROIs were drawn on the axial slices.

The CT images, acquired for attenuation correction, were transferred to Treatment Planning System RayStation 8A (RaySearch Laboratories) to make the volumetric analysis of the ROIs. On each axial slice of CT, a contouring ROI of the structure under examination was created using the tools provided by the software. The system then allowed to view the volumetric result of what was contoured, allowing any changes to be made to the contours, also in coronal and sagittal sections. Finally, the volume of each designed structure was calculated automatically by the software (Fig. **6**).

3. RESULTS

Figs. **7** and **8** show the boxplots and histograms of the error measurements in phantom studies for the three methods. Table **1** shows the corresponding values of the Mean, Median, SD, SE, MAPE and RMSE.

Regarding the planar method, all parameters show higher values than the other two methods. SPECT-CT shows lower variability; in fact, SD, SE and RMSE show the lowest values. Moreover, the MAPE is minimized by the SPECT-CT method. Based on our results, although it is not possible to exclude that SPECT-CT underestimates the volume measurements (p-value = 0.0856 for alternative hypothesis mean less than zero), no significant differences were observed between SPECT and SPECT-CT measurements and weak significance was obtained between planar and SPECT-CT. Statistical significance was calculated through ANOVA (p-value = 0.0784) and post-hoc t.test with Bonferroni correction (planar-SPECT and SPECT-SPECT-CT p-value > 0.5, planar-SPECT-CT p-value = 0.0744). The planar method showed significantly higher values than the gold standard (95% confidence interval for the measurement error = (-0.1038, 1.0496) and p-value = 0.0526 of the t-test for the mean measurement error greater than 0).

Table **2** shows the values of Mean, Median, SD, SE, MAPE and RMSE for the different depths, p and g. Regarding the SPECT-CT method, it is interesting to note that this subanalysis shows lower SD, SE, MAPE and RMSE values for depth p than for depth g.

The volumes measured by means of the three different methods in patient studies are displayed in Table **3**. We considered as relevant percentage differences greater than 20% from the measurements obtained with CT. We found relevant differences in 7 out of 9 lesions with the planar method and in 6 out of 9 with SPECT method, but in only 1 out of 9 lesions with the SPECT-CT method. Moreover, SPECT-CT provided more accurate measurements than the other two methods in 7 out of 9 lesions.

Fig. (5). SPECT-CT axial cross-section with superimposed ROIs obtained automatically by means of a 41% threshold.

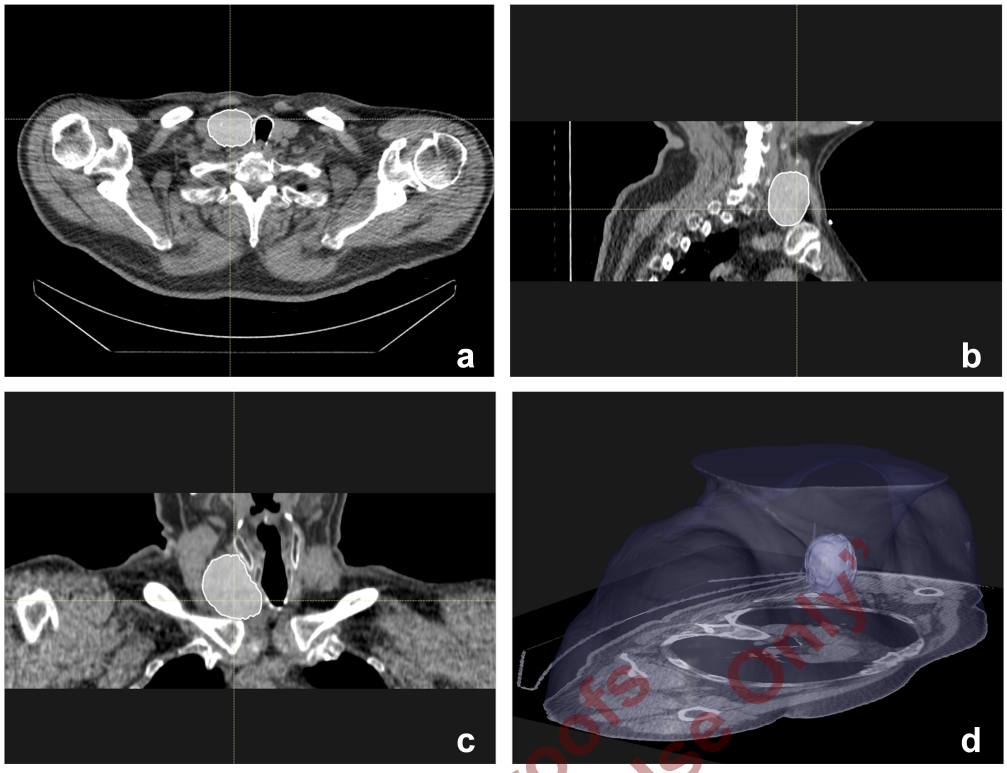

Fig. (6). CT in axial, sagittal and coronal views with corresponding ROIs drawn manually around the nodule of the right thyroid lobe (**a**, **b**, **c**). 3-D rendering of the same lesion is also shown (**d**).

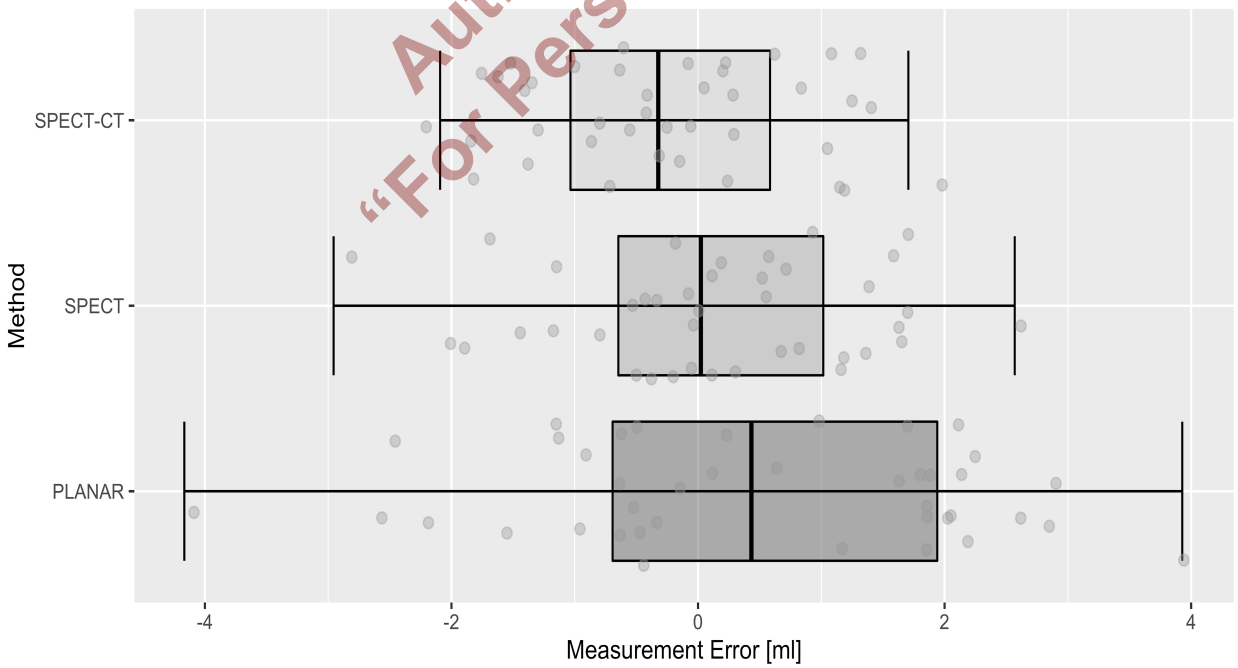

Fig. (7). Boxplots of the measurement errors for the three methods: PLANAR, SPECT and SPECT-CT.

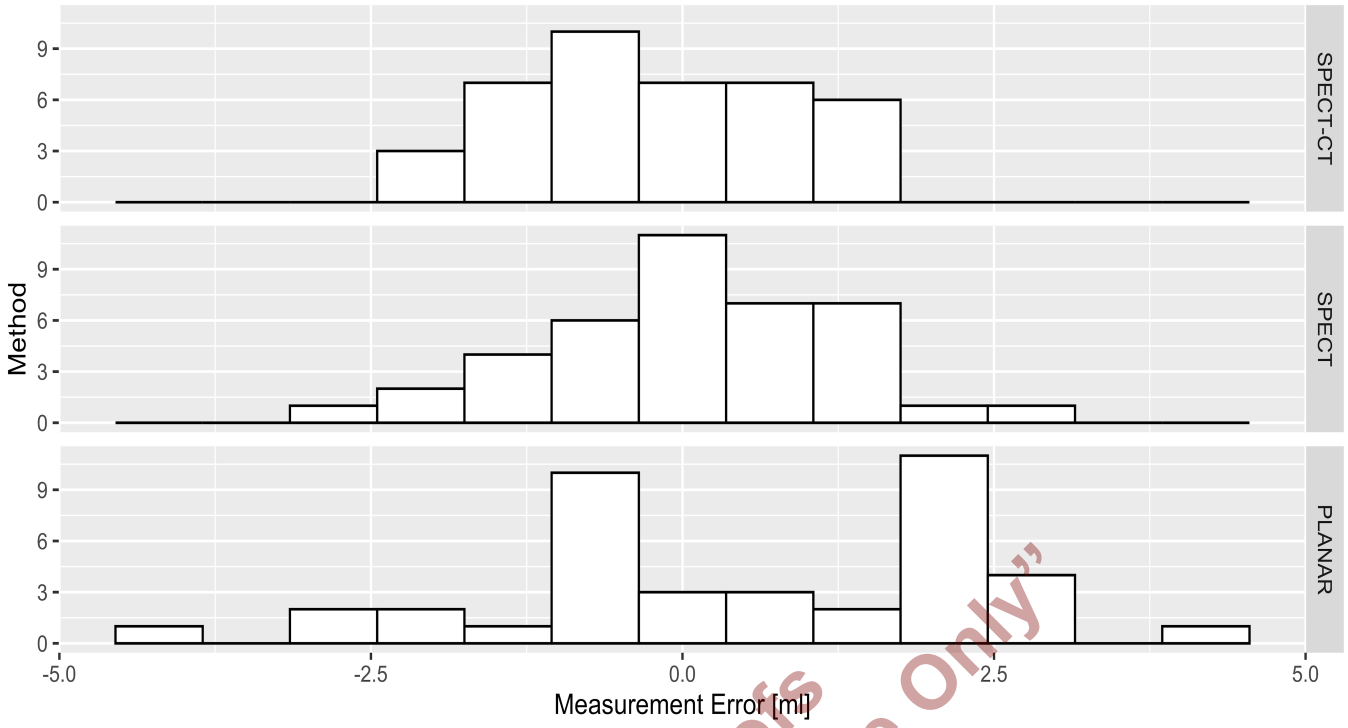

Fig. (8). Histograms of the measurement errors for the three methods: PLANAR, SPECT and SPECT-CT.

Table 1. Mean, Median, SD, MAPE, SE and RMSE of measurement errors for the three methods planar, SPECT and SPECT-CT.

-	PLANAR	SPECT	SPECT-CT
Mean [ml]	0.4729	0.0703	-0.2340
Median [ml]	0.433	0.023	-0.3225
SD [ml]	1.8033	1.1917	1.0618
MAPE [%]	10.3988	6.1867	6.0775
SE [%]	1.9009	1.2562	1.1192
RMSE [ml]	1.8423	1.1788	1.0743

Table 2. Mean, Median, SD, MAPE, SE and RMSE for the two methods SPECT and SPECT-CT and for the two depths p and g.

-	SPECT		SPECT-CT	
-	p	g	p	g
Mean [ml]	0.053	0.0876	-0.1931	-0.275
Median [ml]	-0.02	0.066	-0.193	-0.3655
SD [ml]	1.2573	1.1548	1.0222	1.1251
MAPE [%]	6.5453	5.8280	5.7683	6.3867
SE [%]	1.8743	1.7214	1.5238	1.6771
RMSE [ml]	1.2266	1.1289	1.0149	1.1305

Table 3. Volume measurements in milliliters and percentage difference from the gold standard value obtained by CT for each of the three methods under comparison (planar, SPECT and SPECT-CT).

Patients	Lesion	Target Volume	Planar (ml)	% diff.	SPECT (ml)	% diff.	SPECT-CT (ml)	% diff.	CT (ml)
1	a	ectopic tissue	6.4	-8.05	9.4	35.06	7.16	2.87	6.96
	b	Graves' Disease	10.14	-47.16	14.66	-23.61	21.06	9.74	19.19
2	c	retrosternal hot nodule	29.01	-32.16	34.09	-20.28	40.91	-4.33	42.76
3	d	retrosternal hot nodule	17.87	11.55	10.35	-35.39	16.66	4.00	16.02
4	e	hot nodule	4.57	31.70	4.83	39.19	5.52	59.08	3.47
5	f	hot nodule	18.32	-28.83	22.27	-13.48	22.01	-14.49	25.74
6	g	Graves' Disease	42.59	-30.04	52.22	-14.22	53.43	-12.24	60.88
7	h	Graves' Disease	23.11	-27.92	34.35	7.14	34.18	6.61	32.06
8	i	Graves' Disease	17.37	-52.29	27.88	-23.43	30.55	-16.09	36.41

4. DISCUSSION

Thyroid scintigraphy is a highly sensitive and specific functional imaging that investigates every altered functional state of thyroid conditioning autonomy. It is generally performed with $^{99m}TcO_4^-$ produced by a $^{99}Mo/^{99}Tc$-generator. After intravenous injection, $^{99m}TcO_4^-$ shows a loose bound to plasma proteins and moves rapidly out of the intravascular compartment. Na^+/I^- symporter allows its carriage into the follicular thyroid cell without organification in the gland. The Thyroid Uptake of $^{99m}TcO_4^-$ (TCTU) shows a plateau phase between 15' and 30' minutes. In the geographic areas with sufficient iodine supply, the absolute uptake of $^{99m}TcO_4^-$ ranges from 0.3% and 3% of the administered activity, whereas the range extends from 1.2% to 7% in iodine deficiency areas [13]. TCTU is calculated according to the following formula: TCTU(%) = (counts over thyroid - background counts x)100 / counts of injected activity [14]. Without TSH suppression, TCTU has a limited clinical value. Factors influencing his determination are mainly thyroid volume, iodine supply and patient's age. A substantial overlap of TCTU values can be observed between endemic goiter, euthyroid, thyreotoxic autonomy and Graves' disease. Extreme values are specific respectively for Graves' disease (TCTU > 15%) and iodine contamination (TCTU < 0.3%) [13, 14].

According to the data mentioned above, each vial was filled with a $^{99m}TcO_4^-$ solution in 15 ml of volume, at activity equal to 2%, 4%, 6%, 8% and 10% of 148 MBq, that generally administered for thyroid scintigraphy in adult patients in our Nuclear Medicine Unit. Therefore, a first limit is given by the activity tested in the phantoms, with a range from 0.19 MBq/ml to 0.99 MBq/ml for SPECT and SPECT-CT studies and 0.19 MBq/ml to 0.98 MBq/ml for planar studies.

Regarding the choice of a fixed volume, it is worth mentioning that there is no unanimous consensus in the literature on the normal size of the thyroid in adults obtained by ultrasonography (1). Rumack et al. found a normal adult value of 10-11 ± 3 ml [15]. For Nataf et al. the normal values are > 18 ml for women and > 20 ml for men [16]. Riccabona found normal values below 18 ml in adult males and below 25 ml in adult females but limited to the Austrian population [17]. We have decided to use a fixed volume of 15 ml which, according to the orientation of the liquid in the vial, takes on two different irregular shapes, both akin to a hypertrophic thyroid lobe or a nodular conglomerate. Nevertheless, it represents another limit to the present study in relation to the different impact of the partial volume effect in phantoms of different sizes reported in previous studies, generally consisting of rotation ellipsoids or spheres. Developing a tissue-specific dosimetry method based on planar images, Matheoud et al. [6] introduced in a thyroid phantom three spheres containing ^{123}I in solution, respectively of 10 mm, 13 mm and 16 mm diameter. These authors observed that a partial volume effect needs to be considered for axes ≤ 10 mm, whereas the larger ones were correctly estimated. In our work, we have instead considered phantoms of irregular shape, such that in some parts of them, the thickness was less than 10 mm. This choice was made to evaluate the ability of our SPECT-CT acquisition system to estimate volumes different from a sphere or a rotation ellipsoid since, in clinical practice, the target volume is not always comparable to symmetric geometric shapes. Moreover, we considered also as possible a thickness under one centimeter in relation to the shape of the phantoms used. In particular, phantoms of group B is one centimeter or even less thick for at least one-third of their length.

As a last remark, the neck phantom used in our work does not allow the possibility of having a background activity. As a result, even though rare, this method should not be utilised in clinical cases with poor contrast.

For several decades, radioiodine treatment has been a well-established therapeutic choice in patients with hyperthyroidism due to its safety, effectiveness and low cost. Although the use of fixed doses for the treatment of hyperthyroidism, based on personal experience and literature data, is still common in several Nuclear Medicine Departments, a dosimetry approach in accordance with the ALARA (As Low As Reasonably Achievable) philosophy is nevertheless desirable. The weight of the target mass is among the most

important parameters for the outcome of therapy. Several methods have been proposed for the quantification of the mass of the thyroid gland or the nodules to be given radiometabolic therapy with ^{131}I labeled iodide. They include CT, MR, US, planar scintigraphy, SPECT and PET. In particular, US has generally considered the method of choice for its suitability and cost-effectiveness, but it is based on the assumption that the thyroid nodule or lobes can be approximated by ellipsoids. The inherent uncertainty introduced by this method often exceeds 20%, depending on the shape and size of the target volume. It has been observed that larger errors occur when the measured volume does not correspond to the metabolic active target tissue [18]. Some authors demonstrated the superiority of 3-D US volumetric calculations over 2-D US, especially when a manual tracking method is preferred to the ellipsoid model. These advantages were evident both for regularly shaped phantoms and deformed phantoms. Statistical analysis revealed that sensor navigation and mechanical sweeping techniques were equally suitable for 3-D US [19]. In order to optimize and simplify the diagnostic-therapeutic path, some authors have experienced many methods for measuring the thyroid volume avoiding the dependence on US or other radiological methods. Ronga et al. [20] successfully treated with a single dose of ^{131}I labeled iodide 93% of 1402 patients with solitary thyroid nodule hyperfunctioning, calculating the therapeutic dose through Marinelli formula as simplified by Haines and Keating [21]. The weight of each nodule was estimated palpatory. Besides the considerable experience required, this method of measurement can lead to an overestimation of small nodules and an underestimation of large nodules. In fact, these Authors reported greater responsiveness of small nodules to treatment with respect to larger ones [20].

Different methods of estimating the target volume from the scintigraphy planar image have also been developed. Among the different formulas proposed, the following are worth mentioning: Brämstang's Method (Brämstang, 1968): V = area x 0.75 x b; Modified Brämstang's Method: V = area x c [5]; Lund's Method: V = π / 6 x a x b x c [5, 22], where the delimitation of the cross-sectional area is calculated using a fixed threshold of 10% of the maximum pixel, a and b are respectively the long and the short axis of the ellipse in the anterior planar image, c is the average thickness in a lateral scintigram. Moreover, a reasonable accuracy in volume quantification by SPECT has already been demonstrated. Van Isselt et al. found SPECT a valid alternative to US in the measurement of the thyroid volume in 25 patients with Graves' disease, employing a dual-detector SPECT camera with two gadolinium-153 transmission lines sources. A fix threshold of 45% was used for the segmentation of the gland, as established in patient studies using a Minimal Mean Squared Error method (for SPECT: $R^2 = 0.84$; bias = 1.8 ± 11.9 ml; for US: $R^2 = 0.97$; bias = 6.8 ± 7.5 ml). Planar scintigraphy correlated poorly with MRI ($R^2 = 0.61$) and suffered from a considerable bias (-4 ± 17.6 ml) [9].

The threshold should be adapted to each patient since it depends on various factors, as demonstrated by Mortelmans et al. [23]. In fact, these Authors have verified the dependence on the contrast and on the size of the phantom. Volumes calculated in phantom studies were, instead, very similar with and without the attenuation compensation using a body contour obtained by acquisition of Compton and presuming a constant attenuation factor. With our study, we also demonstrated the dependence of the threshold on the shape of the phantom both in SPECT and in SPECT-CT measurements (Fig. **9**). In this context, it is worth mentioning that the adaptive threshold or grey level histogram method, based on SPECT imaging, can establish the threshold that maximizes the separability of the object from the surround (Otsu, 1979). In the clinical application, the distinction between the class of organ pixels from that of background pixels is not always clear because the valley is not sufficiently deep or because there is a preponderance of one class without any valley [23]. In addition, the method is shown to fail for small volumes where the errors introduced by the partial volume effect are significant [5].

With our method, the calculation of the target volume is simple and quick to achieve. Furthermore, since it is based on an automatic contouring system, it is considered operator-independent essentially. As far as the study on phantoms is concerned, SPECT-CT showed a lower variability with respect to SPECT and even lower with respect to the planar method. The subanalysis conducted for two different depths also showed lower SE and MAPE values for the SPECT-CT at the shallower depth. Furthermore, even though we enrolled only a small number of patients, our study revealed a lower percentage difference in volume estimation in most patients for SPECT-CT with respect to SPECT and planar methods compared to CT gold standard. It is interesting to note that the difference between the two tomographic methods is particularly evident in the case of the ectopic Basedow tissue (lesion "a") and in the two cases in which the target volume was a partially retrosternal hot nodule (lesion "c" and lesion "d"), in addition to a case of Graves' disease (lesion b). In only one case (lesion "e"), the estimated volume was very different from the gold standard for all three methods; this observation could be explained by a greater influence of the partial volume effect in the case of small lesions. Therefore, a CT-based attenuation correction method could be particularly useful for measuring the target volume in cases where tissues of different densities influence the variable attenuation. However, the automatic contouring of the target volume with the software version that we used in the presence of a hyperfunctioning multinodular goiter cannot be applied for lesions with different radiotracer uptake. This can be explained by the fact that the system generates ROIs with a fixed threshold with respect to the point of maximum uptake in the whole series of images. Therefore, an underestimation of the volume occurs in the case of less hyperfunctioning nodules. An underestimation in the measurements may also occur in those cases in which the accumulation of the radiotracer in the salivary glands is greater than in the thyroid nodule. In similar situations, an acidic stimulus could be useful, such as the oral administration of lemon juice.

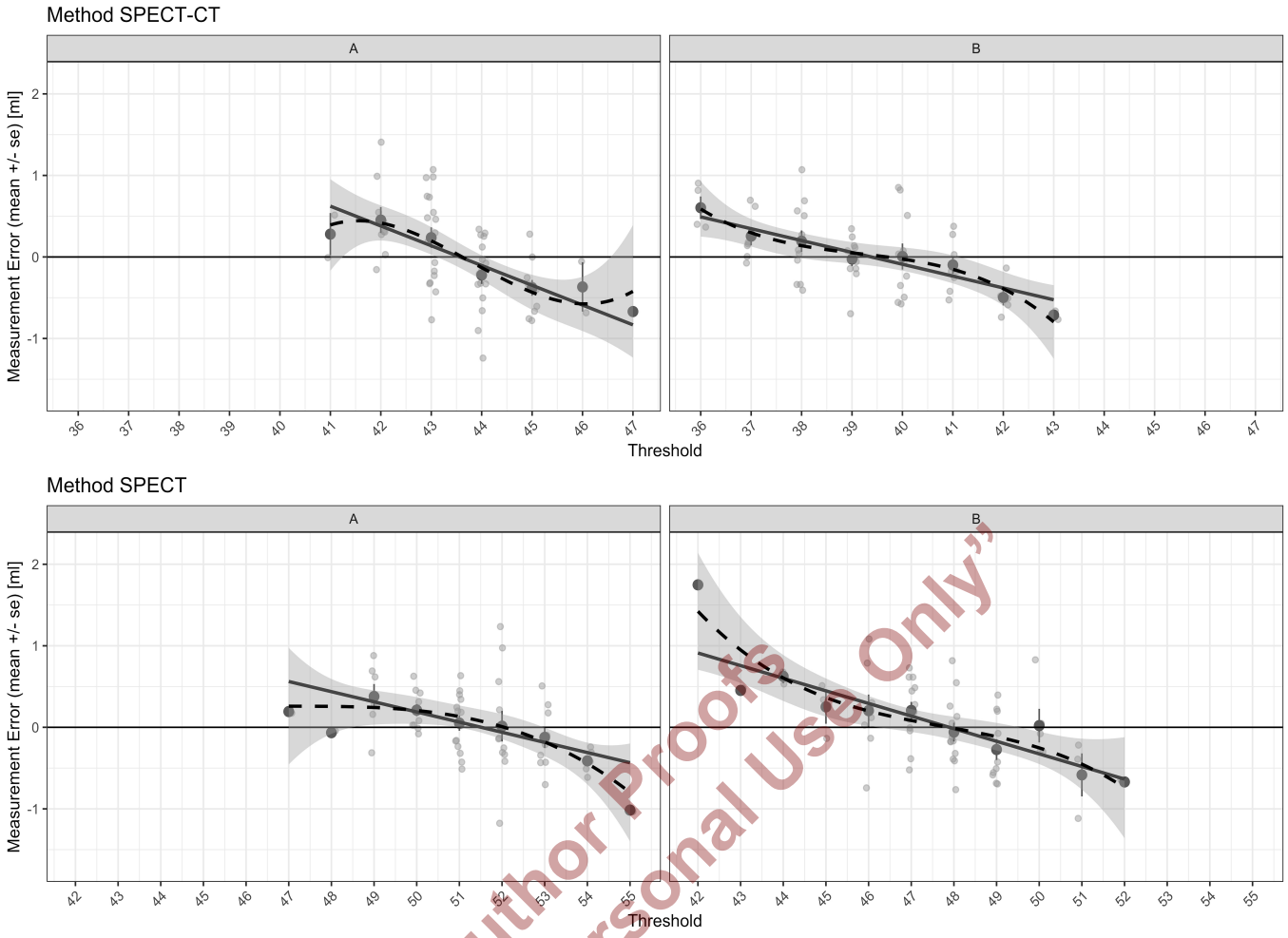

Fig. (9). Linear and spline regression models for the dependency of the volume estimation error on the chosen threshold for the two different shapes of the radioactive liquid, A and B. It is well appreciated the dependence of the threshold on the shape of the phantom both in SPECT and in SPECT-CT measurements.

CONCLUSION

Thyroid tissue volumetry continues to be a challenge in the pre-therapeutic evaluation of radioiodine treatment of hyperthyroidism. Accurate measurement of the target volume is of primary importance in theragnostics of benign thyroid disorders, both for the successful outcome of radioiodine treatment and for lower complications achievable for patients with a calculated dose strategy [24]. Our study confirms the superiority of SPECT in volume measurement if compared with the planar method. A more accurate measurement can be obtained from SPECT-CT, particularly when the tissue to be measured is very deep, as in the case of goiters or retrosternal nodules. In our opinion, the results shown here could encourage further studies in which more patients affected by hyperthyroidism and candidates for radioiodine treatment may be enrolled for a target volume estimation by means of a fixed threshold-based volumetry method from 99mTc-pertechnetate SPECT-CT.

LIST OF ABBREVIATIONS

US	=	Ultrasound
CT	=	Computed Tomography
MR	=	Magnetic Resonance
SPECT-CT	=	Single Photon Emission Computed Tomography - Computed Tomography
SPECT	=	Single Photon Emission Computed Tomography
SD	=	Standard Deviation
SE	=	Standard Error
MAPE	=	Mean Absolute Percentage Error
RMSE	=	Root Mean-Square Error
$^{99m}TcO_4^-$	=	99mTc-pertechnetate

TCTU = Thyroid Uptake of $^{99m}TcO_4^-$

ETHICAL APPROVAL AND CONSENT TO PARTICIPATE

All human procedures were followed in accordance with the ethical standards of the committee responsible for human experimentation (institutional and national). Ethical approval was waived as this included a retrospective study involving data analysis in an anonymous form. All patient data were treated carefully following the Local Privacy Rules and Regulations.

HUMAN AND ANIMAL RIGHTS

No animals were used in this research. The reported experiments were performed in accordance with the ethical standards of the committee responsible for human experimentation (institutional and national) and with the Helsinki Declaration of 1975, as revised in 2013 (http://ethics.iit.edu/ecodes/node/3931).

CONSENT FOR PUBLICATION

Informed consent was obtained from all individual participants included in the study.

STANDARDS OF REPORTING

This paper has been written using STROBE guidelines.

AVAILABILITY OF DATA AND MATERIALS

The datasets used during the current study are available from the corresponding author on a reasonable request.

FUNDING

None.

CONFLICT OF INTEREST

The authors declare no conflict of interest, financial or otherwise.

ACKNOWLEDGEMENTS

Dr. Roberta Maoret and Dr. Leonardo Jon Scotta of Fondazione 3Bi - Biblioteca Biomedica Biellese are gratefully acknowledged for their assistance in bibliographic research.

REFERENCES

[1] Germano, A.; Schmitt, W.; Carvalho, M.R.; Marques, R.M. Normal ultrasound anatomy and common anatomical variants of the thyroid gland plus adjacent structures - A pictorial review. *Clin. Imaging,* **2019**, *58*, 114-128. http://dx.doi.org/10.1016/j.clinimag.2019.07.002 PMID: 31323482

[2] Lee, H.J.; Yoon, D.Y.; Seo, Y.L.; Kim, J.H.; Baek, S.; Lim, K.J.; Cho, Y.K.; Yun, E.J. Intraobserver and interobserver variability in ultrasound measurements of thyroid nodules. *J. Ultrasound Med.,* **2018**, *37*(1), 173-178. http://dx.doi.org/10.1002/jum.14316 PMID: 28736947

[3] Lyshchik, A.; Drozd, V.; Reiners, C. Accuracy of three-dimensional ultrasound for thyroid volume measurement in children and adolescents. *Thyroid,* **2004**, *14*(2), 113-120. http://dx.doi.org/10.1089/105072504322880346 PMID: 15068625

[4] Hanson, M.A.; Shaha, A.R.; Wu, J.X. Surgical approach to the substernal goiter. *Best Pract. Res. Clin. Endocrinol. Metab.,* **2019**, *33*(4)101312 http://dx.doi.org/10.1016/j.beem.2019.101312 PMID: 31477522

[5] Zaidi, H. Comparative methods for quantifying thyroid volume using planar imaging and SPECT. *J. Nucl. Med.,* **1996**, *37*(8), 1421-1426. PMID: 8708788

[6] Matheoud, R.; Canzi, C.; Reschini, E.; Zito, F.; Voltini, F.; Gerundini, P. Tissue-specific dosimetry for radioiodine therapy of the autonomous thyroid nodule. *Med. Phys.,* **2003**, *30*(5), 791-798. http://dx.doi.org/10.1118/1.1567270 PMID: 12772986

[7] Calandri, E.; Filippi, L.; Alessandro, F.; Aretano, I.; Pultrone, M. Usefulness of hybrid single-photon emission computed tomography/ computed tomography in a case of ectopic thyroid tissue in the thyroglossal duct remnant. *Indian J. Nucl. Med.,* **2021**, *36*(1), 97-99. http://dx.doi.org/10.4103/ijnm.IJNM_43_20 PMID: 34040314

[8] Pant, G.S.; Kumar, R.; Gupta, A.K.; Sharma, S.K.; Pandey, A.K. Estimation of thyroid mass in graves' disease by a scintigraphic method. *Nucl. Med. Commun.,* **2003**, *24*(7), 743-748. http://dx.doi.org/10.1097/00006231-200307000-00002 PMID: 12813191

[9] van Isselt, J.W.; de Klerk, J.M.H.; van Rijk, P.P.; van Gils, A.P.G.; Polman, L.J.; Kamphuis, C.; Meijer, R.; Beekman, F.J. Comparison of methods for thyroid volume estimation in patients with graves' disease. *Eur. J. Nucl. Med. Mol. Imaging,* **2003**, *30*(4), 525-531. http://dx.doi.org/10.1007/s00259-002-1101-1 PMID: 12541136

[10] Frangos, S.; Buscombe, J.R. Why should we be concerned about a "g"? *Eur. J. Nucl. Med. Mol. Imaging,* **2019**, *46*(2), 519. http://dx.doi.org/10.1007/s00259-018-4204-z PMID: 30402792

[11] Dottorini, M.E.; Inglese, E.; Salvatori, M.; Signore, A.; Squatrito, S.; Vitti, P. SIE-AIMN-AIFM Guidelines For The Radiometabolic Treatment Of Hyperthyroidism. **2005**. Available from:https://www.aimn.it (Accessed on May 20, 2021).

[12] Hastie, T.; Tibshirani, R.; Friedman, J. *The Elements of Statistical Learning: Data Mining, Inference, and Prediction,* 2nd ed.; Springer Nature, **2013**.

[13] Meller, J.; Becker, W. Scintigraphy with 99mTc-pertechnetate in the evaluation of functional thyroidal autonomy. *Q. J. Nucl. Med.,* **1999**, *43*(3), 179-187. PMID: 10568133

[14] Meller, J.; Becker, W. The continuing importance of thyroid scintigraphy in the era of high-resolution ultrasound. *Eur. J. Nucl. Med. Mol. Imaging,* **2002**, *29 Suppl. 2*, S425-S438. http://dx.doi.org/10.1007/s00259-002-0811-8 PMID: 12192542

[15] Rumack, C.M.; Levine, D. *Diagnostic ultrasound,* 5th ed.; Elsevier: Philadelphia, **2018**.

[16] Nataf., A Figures-benchmarks-measures-classifications in medical imaging. *Sauramps medical: Montpellier,* **2014**.

[17] Riccabona, M. *Pediatric Ultrasound Requisites and Applications,* 2nd ed; Springer: London, **2014**. http://dx.doi.org/10.1007/978-3-642-39156-9

[18] Hänscheid, H.; Canzi, C.; Eschner, W.; Flux, G.; Luster, M.; Strigari, L.; Lassmann, M. EANM dosimetry committee series on standard operational procedures for pre-therapeutic dosimetry II. Dosimetry prior to radioiodine therapy of benign thyroid diseases. *Eur. J. Nucl. Med. Mol. Imaging,* **2013**, *40*(7), 1126-1134. http://dx.doi.org/10.1007/s00259-013-2387-x PMID: 23576099

[19] Freesmeyer, M.; Wiegand, S.; Schierz, J.H.; Winkens, T.; Licht, K. Multimodal evaluation of 2-D and 3-D ultrasound, computed tomography and magnetic resonance imaging in measurements of the thyroid volume using universally applicable cross-sectional imaging software: A phantom study. *Ultrasound Med. Biol.,* **2014**, *40*(7), 1453-1462. http://dx.doi.org/10.1016/j.ultrasmedbio.2014.02.013 PMID: 24768486

[20] Ronga, G.; Filesi, M.; D'Apollo, R.; Toteda, M.; Di Nicola, A.D.; Colandrea, M.; Travascio, L.; Vestri, A.R.; Montesano, T. Autonomous functioning thyroid nodules and 131I in diagnosis and therapy after 50 years of experience: What is still open to debate? *Clin.*

Nucl. Med., **2013**, *38*(5), 349-353.
http://dx.doi.org/10.1097/RLU.0b013e318286bbda PMID: 23531770

[21] Marinelli, L.D.; Quimby, E.H.; Hine, G.J. Dosage determination with radioactive isotopes; Practical considerations in therapy and protection. *Am. J. Roentgenol. Radium Ther.,* **1948**, *59*(2), 260-281.
PMID: 18905884

[22] Olsen, K.J. Scintigraphic estimation of thyroid volume and dose distribution at treatment with 131I. *Acta Radiol. Oncol. Radiat. Phys. Biol.,* **1978**, *17*(1), 74-80.
http://dx.doi.org/10.3109/02841867809127693 PMID: 696403

[23] Mortelmans, L.; Nuyts, J.; Van Pamel, G.; Van den Maegdenbergh, V.; De Roo, M.; Suetens, P. A new thresholding method for volume determination by SPECT. *Eur. J. Nucl. Med.,* **1986**, *12*(5-6), 284-290.
http://dx.doi.org/10.1007/BF00251989 PMID: 3490983

[24] Ariamanesh, S.; Ayati, N.; Khorasani, Z.M.; Mousavi, Z.; Kiavash, V.; Kiamanesh, Z.; Zakavi, S.R. Effect of different 131I dose strategies for treatment of hyperthyroidism on graves' ophthalmopathy. *Clin. Nucl. Med.,* **2020**, *45*(7), 514-518.
http://dx.doi.org/10.1097/RLU.0000000000003086 PMID: 32433165